Journal of Applied Science and Engineering, Vol. 16, No. 2, pp. 165–176 (2013) *DOI: 10.6180/jase.2013.16.2.08*

Unscented Kalman Filtering for Attitude Determination Using MEMS Sensors

Jaw-Kuen Shiau* and I-Chiang Wang

Department of Aerospace Engineering, Tamkang University, Danshui, New Taipei City 25137, Taiwan, R.O.C.

Abstract

This paper presents the results of a quaternion-based unscented Kalman filtering for attitude estimation using low cost MEMS sensors. The unscented Kalman filter uses the pitch and roll angles computed from gravity force decomposition as the measurement for the filter. The immeasurable gravity accelerations are deduced from the outputs of the three axes accelerometers, the relative accelerations, and the accelerations due to body rotation. The constraint of the four elements of the quaternion method is treated as a perfect measurement and is integrated into the system to form a constrained unscented Kalman filter. The heading angle is obtained from a complimentary filter which uses the heading signal derived from the magnetic force information from an electronic magnetic sensor and the GPS-derived heading as the inputs. An experiment using an in-house designed motion platform is conducted to evaluate the proposed algorithm. The noise characteristics of the sensor signals are examined using the laboratory data. Approximations of the time-varying noise variances of the measured signals are obtained through Taylor series expansions. The algorithm is intuitive and easy to implement. Moreover, the proposed algorithm and the filter design are successfully demonstrated through a complete set of flight test data.

Key Words: Flight Information Measurement, Nonlinear Kalman Filter, Quaternion, Complementary Filter

1. Introduction

Obtaining precise attitude information is essential for aircraft navigation and control applications. With the maturation and advancement of semiconductor manufacturing technology, MEMS sensors are increasingly used in flight attitude calculations [1–9]. However, accuracy requirements usually cannot be satisfied by using the inexpensive MEMS sensors. Therefore, some forms of Kalman filtering or complementary fusion algorithms are normally employed to provide more accurate and reliable attitude information in the MEMS attitude determination systems [2–6]. A fuzzy logic based closed-loop strapdown attitude system for UAV is presented in [7]. A miniature MEMS-based attitude and heading reference system, which makes use of an extended Kalman filter with adaptive gain, and with accelerometers and magnetic sensor as the measurements, was presented in [8]. A precision attitude determination employing a multiple model adaptive estimation scheme was reported in [9]. For highly nonlinear systems, the extended Kalman filter may not provide enough accuracy for air vehicle attitude estimation. The unscented Kalman filter will achieve greater attitude estimation performance than the extended Kalman filter through the use of unscented transformation [10–13]. In particular, [10] and [12] demonstrated the success of the unscented Kalman filter design for spacecraft attitude estimation through computer simulation. In [11], an unscented Kalman filter for in-motion alignment of low-cost MEMS-based inertial measurement unit was discussed. It demonstrated that the unscented Kalman filter has the capability to deal

*Corresponding author. E-mail:shiauj@mail.tku.edu.tw

with large and small attitude errors of an inertial navigation system. In [13], an unscented Kalman filter design for attitude estimation of the strapdown inertial navigation system was reported. The simulation results indicated that the performance of the unscented Kalman filter far exceeds the standard extended Kalman filter.

This study considers the development of a quaternion-based unscented Kalman filter for attitude estimation using low-cost MEMS sensors. The filter utilizes the evolution of the four elements in the quaternion method for attitude determination as the dynamic model, with the four elements as the states of the filter. The pitch and roll angles computed from gravity force decomposition are considered as the measurement for the filter. In addition, the constraint of the four elements of the quaternion method is treated as a perfect measurement and is integrated into the filter computation. The immeasurable gravity accelerations are deduced from the outputs of the three axes accelerometers, the relative accelerations, and the accelerations due to body rotation. The source for the heading is different from that for the pitch and roll angles. Therefore we use a complimentary filter to compute the heading angle. The complimentary filter uses the heading signal derived from the magnetic force information from an electronic magnetic sensor and the GPS-derived heading as the inputs to achieve a long-term accurate, reliable and less noisy heading information. An experiment using an in-house designed motion platform is conducted to evaluate the proposed attitude estimation algorithm. The noise characteristics of the sensor signals are examined using the laboratory data. Approximations of the time-varying noise variances of the measured signals are obtained through Taylor series expansions.

The proposed attitude estimation algorithm is demonstrated through a set of flight test data collected from the in-house designed MEMS-based attitude determination system. The duration of the flight covers a total of 3,620 seconds. Details of the evolutions of the attitude angles and some related information such as body axes velocities, angle of attack, and side slip angles are examined and explored in the paper. The results show the long-term stability and practicality of the proposed attitude estimation algorithm.

2. Attitude Determination

The determination of attitude considered in this study is based on a set of signals measured from an in house-designed Flight Information Measurement Unit (FIMU) and a GPS receiver. The basic system structure is shown in Figure 1. The main function of the FIMU system is to measure the essential data required for attitude estimation including the accelerations, angular rates, magnetic fields, and information from the GPS in a real-time and continuous manner. Hence, the navigation computer can use these information to determine the vehicle's attitude. Details of the design and description of the MEMS-based FIMU system can be found in [14].

Determination of flight attitude involves the computation of aircraft pitch angle, roll angle, and heading angle. Pitch angle and roll angle can be computed through the measured aircraft accelerations and body rates from accelerometers and rate gyros. The heading angle is determined by computing the magnetic heading. With the measured three axes acceleration signals and pitch, roll, and yaw rate information – the pitch and roll angles can be determined either by computing the gravitational acceleration components on the body axes, or by using the Euler quaternion method [15]. Computation of the gravitational acceleration components provides long-term accuracy, although it is accompanied by high noise contents. The quaternion method, however, provides low noise contents and fast response to changes in the input signals, but tends to drift with time due to gyro bias errors.

Assume that at a certain instant, the pitch angle of the aircraft is θ, roll angle is ϕ, and the gravitational force components along the body axes (X-, Y-, and Z-axis) are g_x, g_y, and g_z respectively. The relationship between the gravitational acceleration components and the attitude angle are

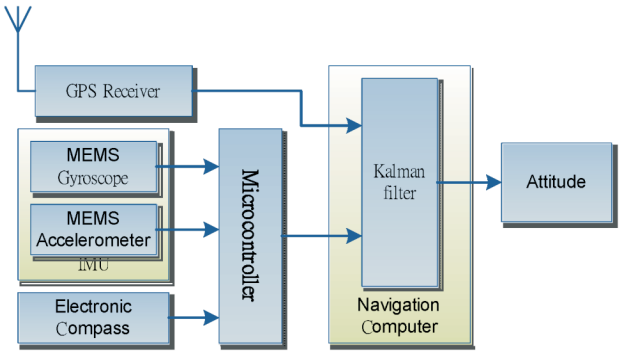

Figure 1. System Structure of the Attitude Estimation System.

$$\begin{bmatrix} g_x \\ g_y \\ g_z \end{bmatrix} = \begin{bmatrix} -g\sin\theta \\ g\sin\phi\cos\theta \\ g\cos\phi\cos\theta \end{bmatrix} \quad (1)$$

With g_x, g_y, and g_z information, the roll angle ϕ and pitch angle θ can be computed from

$$\phi = \tan^{-1}\left(\frac{g_y}{g_z}\right), \quad \theta = \tan^{-1}\left(\frac{-g_x\cos\phi}{g_z}\right) \quad (2)$$

But g_x, g_y, and g_z cannot be measured directly during flight. The immeasurable gravity accelerations can be computed from the outputs of the three axes accelerometers, the relative accelerations, and the accelerations due to body rotation. The accelerations measured from the accelerometers are the total accelerations along the X-, Y-, and Z-axis (a_x, a_y, a_z). The relationship between the measured accelerations (a_x, a_y, a_z) and the gravitational force components are [16]

$$\begin{aligned} a_x &= \dot{U} + (Wq - Vr) + g_x \\ a_y &= \dot{V} + (Ur - Wp) + g_y \\ a_z &= \dot{W} + (Vp - Uq) + g_z \end{aligned} \quad (3)$$

where (U, V, W) are the velocities along the X-, Y-, and Z-axis, whereas (p, q, r) are the pitch rate, roll rate, and yaw rate, respectively.

For magnetic heading computation, assume that the components of the Earth's magnetic field along the X-, Y-, and Z-axis are H_x, H_v and H_z, respectively. Furthermore, the resolved components of H_x, H_v and H_z, in the horizontal plane along the heading axis H_1 and at right angles to the heading axis H_2 are given by [16]

$$H_1 = H_X\cos\theta + H_Y\sin\phi\sin\theta + H_Z\cos\phi\sin\theta \quad (4)$$

$$H_2 = H_Y\cos\phi - H_Z\sin\phi \quad (5)$$

Thus, the magnetic heading of the aircraft ψ_M is

$$\psi_M = \tan^{-1}\frac{H_2}{H_1} \quad (6)$$

If the local magnetic declination is ψ_{md}, the measured aircraft heading, ψ_m, can be determined from $\psi_m = \psi_M + \psi_{md}$. In this computation, the pitch angle θ and roll angle ϕ are assumed to be known. That is, we have to estimate θ and ϕ first before computing the aircraft heading.

A common method used to compute the attitude angle in inertial navigation system is the Euler quaternion method [16], which uses the Euler four symmetrical parameters (e_0, e_1, e_2, e_3) to define the aircraft attitude. The relationship between the attitude angle and the four parameters are

$$\begin{bmatrix} \phi \\ \theta \\ \psi \end{bmatrix} = \begin{bmatrix} \tan^{-1}\left(\frac{2(e_0e_1 + e_2e_3)}{e_0^2 - e_1^2 - e_2^2 + e_3^2}\right) \\ \sin^{-1}2(e_0e_3 - e_1e_2) \\ \tan^{-1}\left(\frac{2(e_0e_3 + e_1e_2)}{e_0^2 + e_1^2 - e_2^2 + e_3^2}\right) \end{bmatrix} \quad (7)$$

The four parameters are subjected to the following constraint equation

$$e_0^2 + e_1^2 + e_2^2 + e_3^2 = 1 \quad (8)$$

The dynamics of the four parameters regarding the aircraft body rate (p, q, r) are characterized by the following form:

$$\begin{bmatrix} \dot{e}_0 \\ \dot{e}_1 \\ \dot{e}_2 \\ \dot{e}_3 \end{bmatrix} = 0.5\cdot\begin{bmatrix} 0 & -p & -q & -r \\ p & 0 & r & -q \\ q & -r & 0 & p \\ r & q & -p & 0 \end{bmatrix}\begin{bmatrix} e_0 \\ e_1 \\ e_2 \\ e_3 \end{bmatrix} \quad (9)$$

Therefore, the attitude angles in (7) may be calculated by solving Equation (9). Only body information – (p, q, r) directly measured from rate gyros – is required to solve Equation (9). However, when MEMS gyros are used for body rate measurement, long-term drift usually encountered due to gyro bias errors and integral operation for solving Equation (9).

3. Unscented Kalman Filter Design

In this study, the measured pitch and roll angles are deduced from the outputs of the accelerometers, gyros, and the GPS receiver while the heading angle is from the electronic compass unit. To simplify the design, two filters are designed for the attitude estimation. The pitch and roll angles are determined based on a constrained unscented Kalman filter. The heading angle estimation is

achieved through a complimentary filter. Design of a complementary filter for the single variable – heading, is relatively easier than the design for filtering the coupling variables – pitch and roll angles. Therefore we concentrate on the development of a constrained unscented Kalman filter in this paper.

As discussed in the previous section, the pitch and roll angles computed from the gravitational force components provide long-term accuracy with high noise contents. The Euler quaternion method, however, provides less noisy results but suffers from a long-term drift problem. Either method alone may be inadequate for attitude computation. Hence, in this study, the unscented Kalman filter [17] is implemented to integrate the attitude computation from the gravitational force components and from the Euler quaternion method.

The Kalman filter is a model-based estimation technique. The dynamics that characterize the relationship between the aircraft body rate (pitch, roll, and yaw rates) and the four parameters of the quaternion method described in Equation (9) comprises the dynamic model of the Kalman filter. The relationship between the attitude angle and the four parameters in (7) is chosen as the output equation of the filter. Thus, the dynamic system can be expressed as

$$\begin{aligned} \dot{x} &= Ax + w \\ y &= h(x) + v \end{aligned} \tag{10}$$

where $x = [e_0 \ e_1 \ e_2 \ e_3]^T$ is the state of the system, $y = [\phi \ \theta \ 1]^T$ is *t*he output, and w and ν are the precess and measurement noise, respectively. The system matrix A and output function $h(x)$ are defined as

$$A = \begin{bmatrix} 0 & -\frac{p}{2} & -\frac{q}{2} & -\frac{r}{2} \\ \frac{p}{2} & 0 & \frac{r}{2} & -\frac{q}{2} \\ \frac{q}{2} & -\frac{r}{2} & 0 & \frac{p}{2} \\ \frac{r}{2} & \frac{q}{2} & -\frac{p}{2} & 0 \end{bmatrix}; \ h(x) = \begin{bmatrix} \tan^{-1}\left(\frac{2(e_0e_1 + e_2e_3)}{e_0^2 - e_1^2 - e_2^2 + e_3^2}\right) \\ \sin^{-1} 2(e_0e_3 - e_1e_2) \\ e_0^2 + e_1^2 + e_2^2 + e_3^2 \end{bmatrix} \tag{11}$$

The measurements of pitch angle θ and roll angle ϕ are determined from the gravitation force components in (1). The gravitation force components (g_x, g_y, g_z) are determined from (3), that is

$$\begin{aligned} g_x &= a_x - [\dot{U} + (Wq - Vr)] \\ g_y &= a_y - [\dot{V} + (Ur - Wp)] \\ g_z &= a_z - [\dot{W} + (Vp - Uq)] \end{aligned} \tag{12}$$

Besides the measurement of accelerations (a_x, a_y, a_z) and body rates (p,q,r), the velocities (U, V, W) and velocities' rates ($\dot{U}, \dot{V}, \dot{W}$) along the body axes are also required. The velocities (U, V, W) are determined from the ground speed information (V_N, the north velocity, V_E, the east velocity, and V_D, the down velocity of the aircraft) from the GPS receiver through yaw, pitch, and roll rotation sequence. Equation (13) expresses the coordinate transformation for (V_N, V_E, V_D) and (U, V, W).

$$\begin{bmatrix} U \\ V \\ W \end{bmatrix} = R_{\psi\theta\phi} \begin{bmatrix} V_N \\ V_E \\ V_D \end{bmatrix} \tag{13}$$

The transformation matrix $R_{\psi\theta\phi}$ is defined as

$$\begin{aligned} R_{\psi\theta\phi} &= \begin{bmatrix} 1 & 0 & 0 \\ 0 & \cos\phi & \sin\phi \\ 0 & -\sin\phi & \cos\phi \end{bmatrix} \begin{bmatrix} \cos\theta & 0 & -\sin\theta \\ 0 & 1 & 0 \\ \sin\theta & 0 & \cos\theta \end{bmatrix} \begin{bmatrix} \cos\psi & \sin\psi & 0 \\ -\sin\psi & \cos\psi & 0 \\ 0 & 0 & 1 \end{bmatrix} \\ &= \begin{bmatrix} \cos\psi\cos\theta & \sin\psi\cos\theta & -\sin\theta \\ -\sin\psi\cos\phi + \cos\psi\sin\theta\sin\phi & \cos\psi\cos\phi + \sin\psi\sin\theta\sin\phi & \cos\theta\sin\phi \\ \sin\psi\sin\phi + \cos\psi\sin\theta\cos\phi & -\cos\psi\sin\phi + \sin\psi\sin\theta\cos\phi & \cos\theta\cos\phi \end{bmatrix} \end{aligned} \tag{14}$$

Similarly, the velocities' rates ($\dot{U}, \dot{V}, \dot{W}$) is computed from

$$\begin{bmatrix} \dot{U} \\ \dot{V} \\ \dot{W} \end{bmatrix} = R_{\psi\theta\phi} \begin{bmatrix} \dot{V}_N \\ \dot{V}_E \\ \dot{V}_D \end{bmatrix} \tag{15}$$

For real time computation, the dynamical system (10) is expressed in discrete time representation as

$$\begin{aligned} x(k+1) &= F(k)x(k) + w(k) \\ y(k) &= h[x(k)] + v(k) \end{aligned} \tag{16}$$

where $F(k) = e^{A\Delta T}$, which can be approximated by

$$F(k) = \begin{bmatrix} 1 & -\frac{p(k)\Delta T}{2} & -\frac{q(k)\Delta T}{2} & -\frac{r(k)\Delta T}{2} \\ \frac{p(k)\Delta T}{2} & 1 & \frac{r(k)\Delta T}{2} & -\frac{q(k)\Delta T}{2} \\ \frac{q(k)\Delta T}{2} & -\frac{r(k)\Delta T}{2} & 1 & \frac{p(k)\Delta T}{2} \\ \frac{r(k)\Delta T}{2} & \frac{q(k)\Delta T}{2} & -\frac{p(k)\Delta T}{2} & 1 \end{bmatrix} \tag{17}$$

The sampling time ΔT is 0.05 seconds in this study.

The attitude estimation problem in this study is nonlinear and time varying. It is usually difficult to transform the probability density function (pdf) of the mean and covariance of a random variable through a general nonlinear function. The unscented transformation is an effective way to approximate how the mean and covariance of a random variable change when it undergoes a nonlinear transformation. It is based on the facts that performing a nonlinear transformation on a single point is easy and it is not to hard to to find a set of individual points in state space whose sample pdf approximates the true pdf of a state vector [17]. Thus, if we know the mean $\bar{x}$ and covariance P of a vector x, we can find a set of deterministic vectors called sigma points whose ensemble mean and covariance are equal to $\bar{x}$ and P. These obtained sigma points are used to generate a set of transformed vectors through the nonlinear function $y = h(x)$. The ensemble mean and covariance of the transformed vectors will provide a good estimate of the true mean and covariance of the random variable y. Suppose the random variable x is a $n \times 1$ vector with mean $\bar{x}$ and covariance P, we can choose 2n sigma points $x^{(i)}$ as follows:

$$\begin{aligned} x^{(i)} &= \bar{x} + \tilde{x}^{(i)} \qquad i = 1, \cdots, 2n \\ \tilde{x}^{(i)} &= (\sqrt{nP})_i^T \qquad i = 1, \cdots, n \\ \tilde{x}^{(n+i)} &= -(\sqrt{nP})_i^T \qquad i = 1, \cdots, n \end{aligned} \tag{18}$$

where $\sqrt{nP}$ is the matrix square root of nP and $(\sqrt{nP})_i$ is the ith row of $\sqrt{nP}$. The unscented transformation will provide more accurate mean and covariance than those from the linearized transformation. The unscented Kalman filters use the unscented transformations for propagating means and covariances. In this study, the state variable is $x = [e_0, e_1, e_2, e_3]^T$, that is $n = 4$. Thus, eight sigma points are selected for the unscented transformation.

The details of the computation process for the attitude estimation algorithm proposed in this study are depicted in Figure 2, and the unscented Kalman filtering details are presented in Figure 3. As indicated in Figure 3, the covariances of the process noise Q_{k-1} and the measurement noise R_k are required in estimating the a priori error covariance P_k^- and the covariance of the predicted measurement P_y. The process noises are mainly derived from the outputs of the gyros (p, q, r). Assuming that $p = \bar{p} + \tilde{p}$, $q = \bar{q} + \tilde{q}$, and $r = \bar{r} + \tilde{r}$ with $\bar{p}, \bar{q}$, and $\bar{r}$ the mean of p, q, and r respectively, and $\tilde{p}$, $\tilde{q}$, and $\tilde{r}$ are the deviations of p, q, and r, Equation (9) can be written as

$$\begin{bmatrix} \dot{e}_0 \\ \dot{e}_1 \\ \dot{e}_2 \\ \dot{e}_3 \end{bmatrix} = \frac{1}{2} \cdot \begin{bmatrix} 0 & -(\bar{p}+\tilde{p}) & -(\bar{q}+\tilde{q}) & -(\bar{r}+\tilde{r}) \\ (\bar{p}+\tilde{p}) & 0 & (\bar{r}+\tilde{r}) & -(\bar{q}+\tilde{q}) \\ (\bar{q}+\tilde{q}) & -(\bar{r}+\tilde{r}) & 0 & (\bar{p}+\tilde{p}) \\ (\bar{r}+\tilde{r}) & (\bar{q}+\tilde{q}) & -(\bar{p}+\tilde{p}) & 0 \end{bmatrix} \begin{bmatrix} e_0 \\ e_1 \\ e_2 \\ e_3 \end{bmatrix}$$

$$= \frac{1}{2} \cdot \begin{bmatrix} 0 & -\bar{p} & -\bar{q} & -\bar{r} \\ \bar{p} & 0 & \bar{r} & -\bar{q} \\ \bar{q} & -\bar{r} & 0 & \bar{p} \\ \bar{r} & \bar{q} & -\bar{p} & 0 \end{bmatrix} \begin{bmatrix} e_0 \\ e_1 \\ e_2 \\ e_3 \end{bmatrix} + \frac{1}{2} \begin{bmatrix} -e_1 & -e_2 & -e_3 \\ e_0 & -e_3 & e_2 \\ e_3 & e_0 & -e_1 \\ -e_2 & e_1 & e_0 \end{bmatrix} \begin{bmatrix} \tilde{p}(t) \\ \tilde{q}(t) \\ \tilde{r}(t) \end{bmatrix}$$

The second term on the right hand side is considered as the process noise $w(t)$ in this study. The process noise $w(t)$ in discrete representation, denoted as $w(t)$, is

$$w(k) = \frac{1}{2} \begin{bmatrix} -e_1 & -e_2 & -e_3 \\ e_0 & -e_3 & e_2 \\ e_3 & e_0 & -e_1 \\ -e_2 & e_1 & e_0 \end{bmatrix} \begin{bmatrix} \tilde{p}(k) \\ \tilde{q}(k) \\ \tilde{r}(k) \end{bmatrix} \tag{19}$$

It is simple to show that the variance of the process noise Q_{k-1} is $L_{k-1}\tilde{Q}_{k-1}L_{k-1}^T$ with

$$L_{k-1} = \frac{1}{2} \begin{bmatrix} -e_1 & -e_2 & -e_3 \\ e_0 & -e_3 & e_2 \\ e_3 & e_0 & -e_1 \\ -e_2 & e_1 & e_0 \end{bmatrix}, \quad \tilde{Q}_{k-1} = \begin{bmatrix} \sigma_p^2 & 0 & 0 \\ 0 & \sigma_q^2 & 0 \\ 0 & 0 & \sigma_r^2 \end{bmatrix} \tag{20}$$

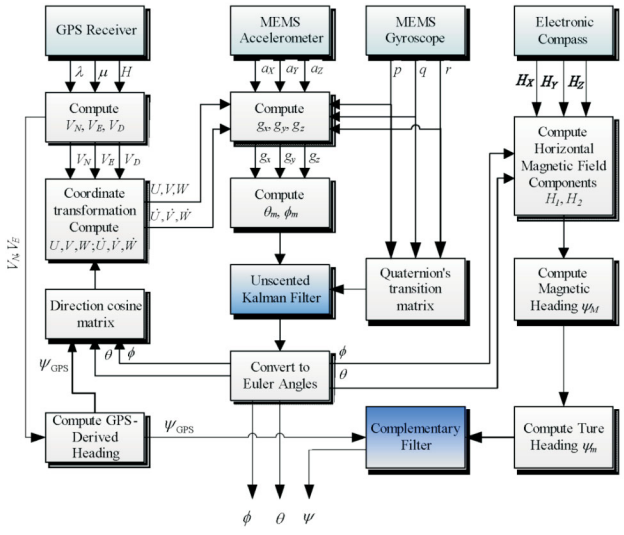

Figure 2. Computation process for attitude estimation

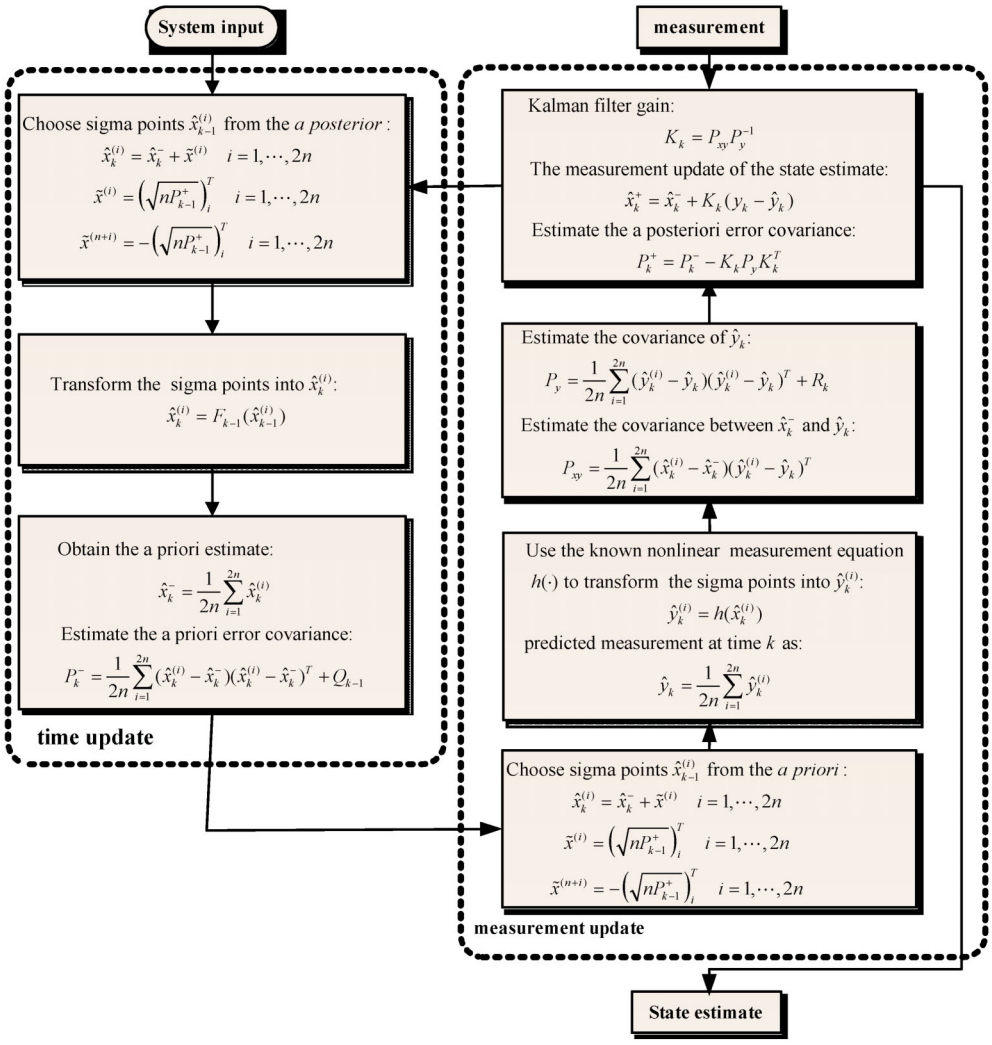

Figure 3. Unscented Kalman Filtering.

where σ_p^2, σ_q^2, and σ_r^2 are the variances of p, q, and r, respectively.

The characteristics of the sources of the measurement determine the variances of the measurement noises. The roll angle ϕ and pitch angle θ are computed from

$$\phi = \tan^{-1}\left(\frac{g_y}{g_z}\right), \quad \theta = \tan^{-1}\left(\frac{-g_x \cos\phi}{g_z}\right) \tag{21}$$

The deviations of ϕ and θ can be decided by expanding (21) in a Taylor series about the mean of the measured variables, (a_x, a_y, a_z), (U, V, W), ($\dot{U}$,$\dot{V}$,$\dot{W}$), (p, q, r) and neglecting the second order terms. After a tedious derivation, the covariance of the measurement noise R_k can be expressed as

$$R_k = M_{\phi\theta} M_{xyz} R_{\phi\theta} M_{xyz}^T M_{\phi\theta}^T \tag{22}$$

where

$$M_{\phi\theta} = \begin{bmatrix} 0 & \frac{g_z}{g_y^2 + g_z^2} & -\frac{g_y}{g_y^2 + g_z^2} \\ \frac{-g_z \cos\phi}{g_x^2 \cos^2\phi + g_z^2} & \frac{g_x g_z^2 \sin\phi}{(g_y^2 + g_z^2)(g_x^2 \cos^2\phi + g_z^2)} & \frac{(g_y^2 + g_z^2) g_x \cos\phi - g_x g_y g_z \sin\phi}{(g_y^2 + g_z^2)(g_x^2 \cos^2\phi + g_z^2)} \end{bmatrix} \tag{23}$$

$$M_{xyz} = \begin{bmatrix} 1 & 0 & 0 & -1 & 0 & 0 & 0 & r & -q & 0 & -W & V \\ 0 & 1 & 0 & 0 & -1 & 0 & -r & 0 & p & W & 0 & -U \\ 0 & 0 & 1 & 0 & 0 & -1 & q & -p & 0 & -V & U & 0 \end{bmatrix} \tag{24}$$

$$R_{\phi\theta} = diag[\sigma^2_{a_x} \quad \sigma^2_{a_Y} \quad \sigma^2_{a_Z} \quad \sigma^2_{\dot{U}} \quad \sigma^2_{\dot{V}} \quad \sigma^2_{\dot{W}} \quad \sigma^2_{U} \quad \sigma^2_{V} \quad \sigma^2_{W} \quad \sigma^2_{p} \quad \sigma^2_{q} \quad \sigma^2_{r}] \tag{25}$$

and σ^2_{φ} represents the variance of the signal φ. Significantly, in (25) all noise sources are assumed to be uncorrelated. With all of these information the pitch and roll angles can be estimated. Utilizing the estimated pitch and roll angles the heading angle is computed through a second order complementary filter. The complementary filter uses the heading signal derived from the measured magnetic force information and the GPS-derived heading as the inputs to achieve a long-term accurate, reliable and less noisy heading information. The filtering system adopted in this design is

$$\psi = \frac{2\zeta\omega_0 s + \omega_0^2}{s^2 + 2\zeta\omega_0 s + \omega_0^2}\psi_m + \frac{s^2}{s^2 + 2\zeta\omega_0 s + \omega_0^2}\psi_{GPS} \tag{26}$$

with $\zeta = 1$ and $\omega_0 = 0.4\pi$. The measured ψ_m is the magnetic heading corrected with local magnetic declination and is accompanied by high noise contents. The GPS-derived heading ψ_{GPS} is computed from

$$\psi_{GPS} = \tan^{-1}\left(\frac{V_E}{V_N}\right) \tag{27}$$

The GPS-derived heading is assumed to be subjected to prevailing wind effect.

4. Laboratory Test

Because there is no primary standard, the proposed attitude estimation algorithm is tested using a motion platform under a controlled environment to evaluate performance of the proposed algorithm. An image of the motion platform and the test arrangement is shown in Figure 4. A cantilever beam is mounted atop the motion platform. A movable mounting plate is constructed at the end of the beam. The movable mounting plate can be turn to and fixed at a pre-selected angle measured from the horizontal plane. A MEMS-based inertial measurement unit (IMU) is placed on the specially designed mounting plate. The orientation of the IMU measurement is as defined in Figure 4. An on-board computer is mounted on top of the center of the motion platform to record the outputs from the IMU during the test.

The motion platform is controlled to perform uniform circular motion. The parameters selected to perform the test are listed in Table 1. The rotating radius, 0.64 m, in Table 1 is the distance from the center of the IMU to the rotating axis. The IMU is mounted with 0 degree pitch angle and -20 degrees roll angle. Since the angular velocity and the rotating radius are fixed, the velocities (U, V, W) and accelerations ($\dot{U}, \dot{V}, \dot{W}$) along the body axes of the IMU can be determined directly.

For uniform circular motion with the parameters set in Table 1, the velocities (U, V, W) and accelerations ($\dot{U}, \dot{V}, \dot{W}$) are U = 0.4466 m/sec, $V = W = 0$ m/sec, and $\dot{U} = \dot{V} = \dot{W} = 0\,\text{m/sec}^2$. Using these velocity and acceleration information together with the accelerations measured from the accelerometers and the body rates from the gyro outputs, the pitch angle and roll angle can be determine from the gravity force components or from the Euler quaternion method. The results from the gravity force decomposition are shown in Figure 5. The results in Figure 5 indicate that the gravity force decomposition will provide accurate results of 0 degree pitch angle and -20 degrees roll angle but suffer from noisy contents. The results from Euler quaternion method are shown in Figure 6. In Figure 6, roll angle is correctly deduced

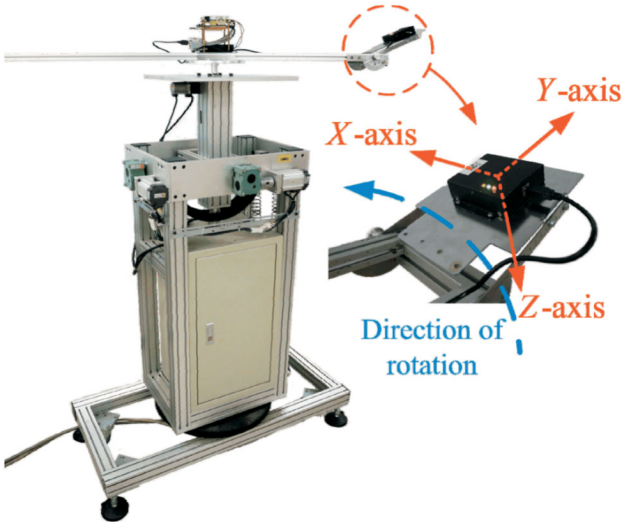

Figure 4. The motion platform and the test arrangement

Table 1. Parameters for the Lab test

angular velocity ω	rotating radius R	Pitch angle θ	Roll angle ϕ
0.873 (rad/sec)	0.64 (m)	0°	-20°

from the quaternion computation with less noisy contents. However, the pitch angle tends to diverge. The results using the proposed unscented Kalman filtering are presented in Figure 7. It provides both accurate and less noisy results for the pitch and roll angles.

5. Evaluation Using Flight Test Data

To verify the practicality of attitude estimation algorithm presented in the paper, the algorithm is tested using a complete set of flight test data from an ultra-light aircraft. A flight test was conducted using an ultra-light aircraft as the test bed with the MEMS-based Flight Information Measurement Unit installed on the aircraft. The field data, taken from an in-house designed MEMS-based Flight Information Measurement Unit, includes the three axes body rates (p, q, r), accelerations (a_x, a_y, a_z), magnetic field (H_X, H_Y, H_Z), and information from GPS receiver. The flight was performed in Central Taiwan at approximately 120.44 degrees East Longitude and 23.77 degrees North Latitude area. The weather was clear with wind roughly from the north. The airplane flew in the low altitude region. Thus the horizontal component of the wind would be the major part to affect the aircraft operation. The flight trajectory is shown in Figure 8. The evolutions of the attitude, including pitch, roll, and heading angles are shown in Figure 9. The attitude angles (directly generated from the measured data and computed after filtering) are both shown in Figure 9. The duration of the flight covers a total of 3,620 seconds. The results are further examined and discussed below. Much

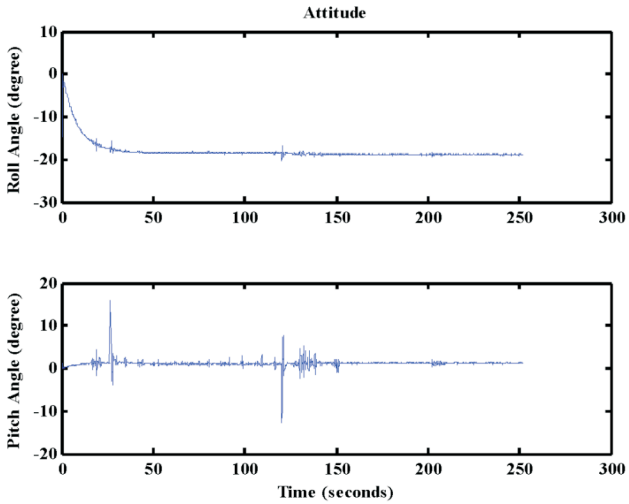

Figure 5. Attitude determination using gravity component method.

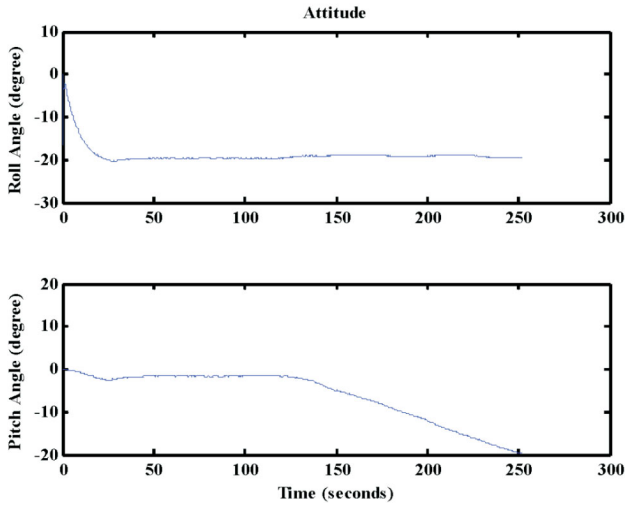

Figure 6. Attitude determination using quaternion method.

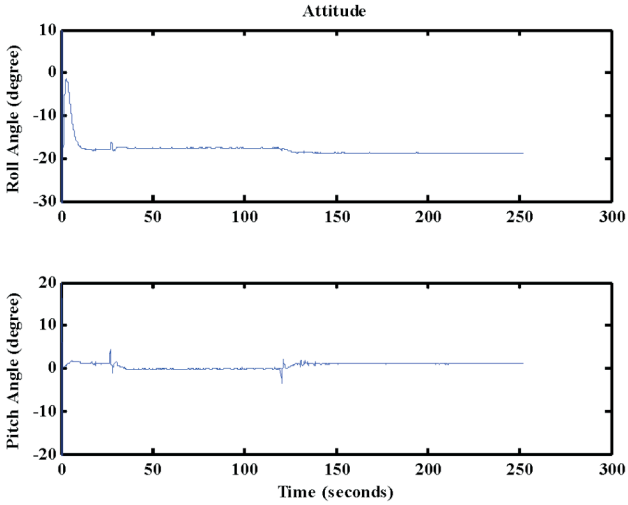

Figure 7. Attitude determination using unscented Kalman filter.

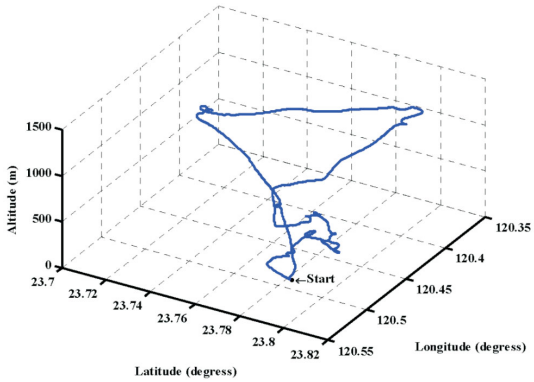

Figure 8. Trajectory of the complete flight.

of the noisy signals of the attitude angles in the followings figures are the results deduced from the measurement, whereas the less noisy signals are the results of the filtered signals.

The results for the climbing up condition are shown in Figures 10–12. During the time period of 1,420 to 1,430 seconds, the airplane climbed from 1,009 m to 1,019 m height. Figure 10(d) indicates that the heading was around 0 degrees. That is, the airplane flew to the north during this period. The velocities (*U*, *V*, *W*) along the body axes are recomputed using equation (14) after the attitude estimation and are shown in Figure 11. The lateral velocity *V* in Figure 11 is around zero because the wind was from the north. Figure 12 is the result for the computed angle of attack α and angle of sideslip. Nearly zero sideslip angles confirm that the wind is from the north. The results for nearly level flight with wing wiggling (intentionally commanded) are shown in Figures 13–15. In this phase, the altitude was sustained at approximately 392 to 393 meters height, as shown in Figure 13(a). The roll angle, as shown in Figure 13(c), responded as commanded. Figure 13(d) shows the tendency of turning to the left. The average of the roll angles in Figure 13(c) is negative, which confirms that the airplane is turning left slowly. The lateral velocity *V* in Figure 14 and sideslip angle β in Figure 15 are both positive due to the effect of the north wind.

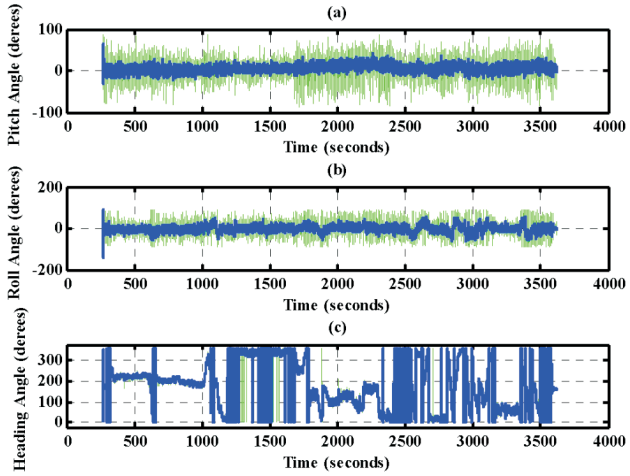

Figure 9. Evolutions of the attitude angles. The much noisy signals are the results deduced from the measurement, whereas the less noisy signals are the results of the filtered signals.

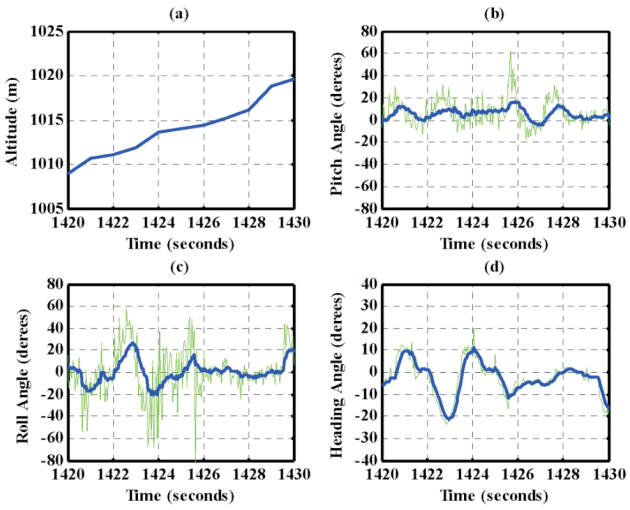

Figure 10. Attitude for climbing-up condition. The much noisy signals are the results deduced from the measurement, whereas the less noisy signals are the results of the filtered signals.

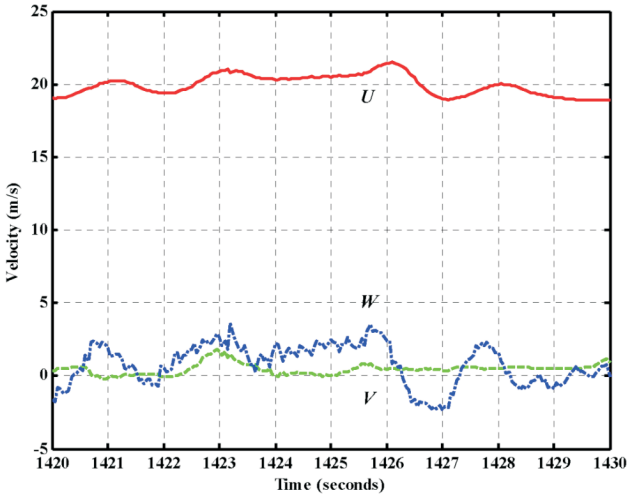

Figure 11. Velocities along body axes (1420–1430 sec).

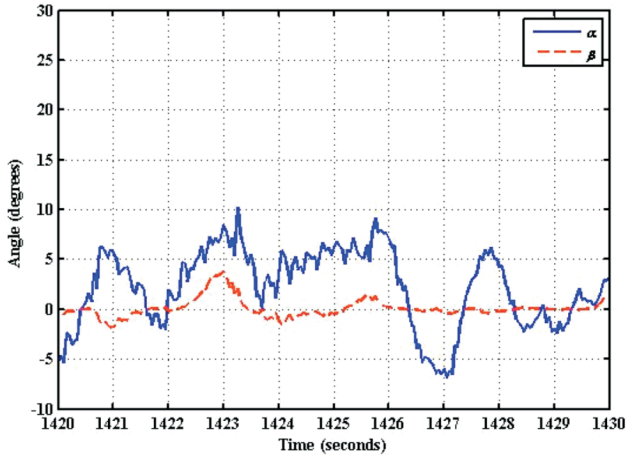

Figure 12. Angle of attack and angle of sideslip (1420–1430 sec).

During the time period from 2,810 to 2,900 seconds, the airplane made an S-turn. Evolutions of the attitude angles during this maneuver are shown in Figure 16. Figure 16(a) shows the trajectory of the S-turn maneuver from the GPS data. The arrow in Figure 16(a) shows the direction of flight. During this particular maneuver, the airplane makes a left turn before following with a right turn. Figure 16(c) shows that the roll angle turns to a negative value first, then returns to zero degrees for the left maneuver, which verifies that the airplane was making a left turn. Thereafter, it turns positive before returning to zero degrees for a right turning operation. The heading angle shown in Figure 16(d) starts from approximately 340 degrees and gradually decreases to roughly 25 degrees, then increases back to 335 degrees, which correctly corresponds to the S-turn operation. Figures 17 and 18 are the corresponding body axes velocities (U, V, W) and the angle of attack and sideslip angles during this particular maneuver.

From the above examinations, we verified that the proposed attitude determination algorithm estimates the attitude angles successfully. The algorithm is also reliable for long-term and high-dynamic maneuvers.

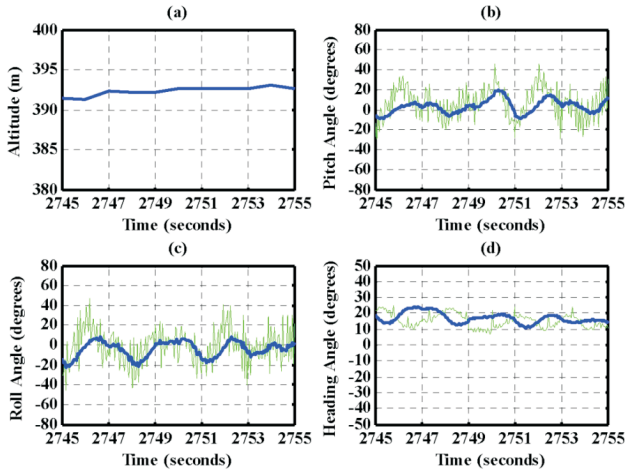

Figure 13. Nearly level flight with wing wiggling. The much noisy signals are the results deduced from the measurement, whereas the less noisy signals are the results of the filtered signals.

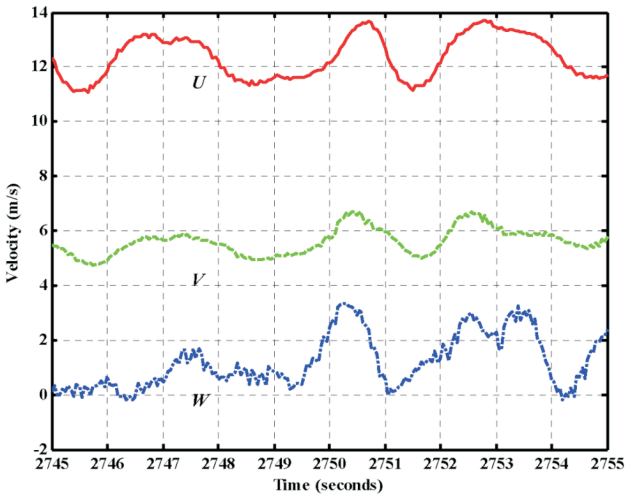

Figure 14. Velocities along body axes (2745–2755 sec).

6. Conclusions

This study presented a constrained unscented Kal-

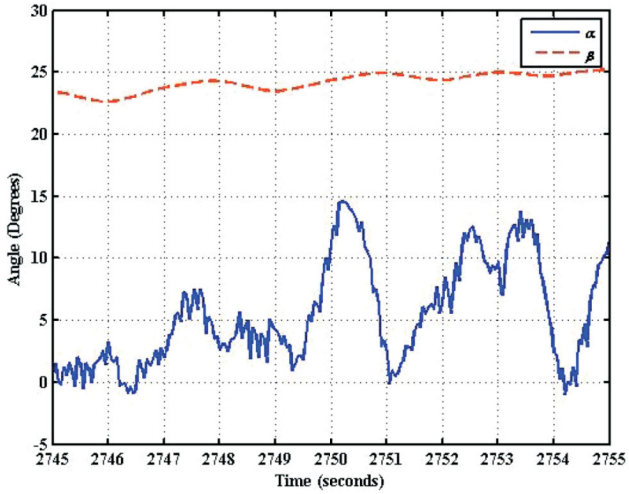

Figure 15. Angle of attack α and angle of sideslip β (2745–2755 sec).

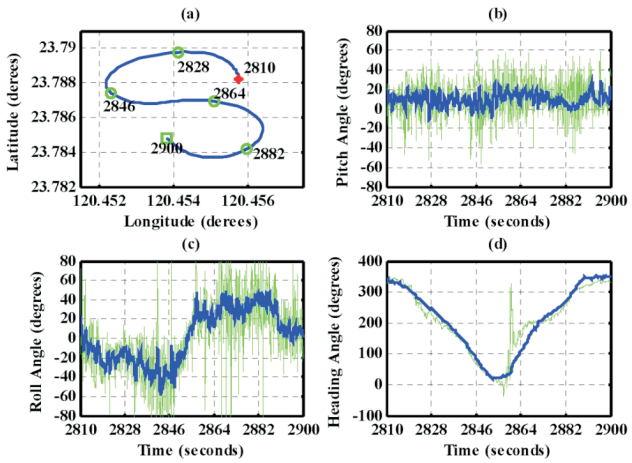

Figure 16. Attitude evolutions during an S-turn maneuver. The much noisy signals are the results deduced from the measurement, whereas the less noisy signals are the results of the filtered signals.

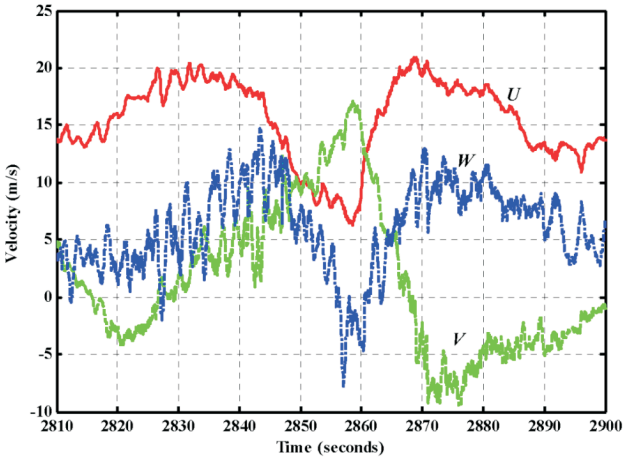

Figure 17. Velocities along body axes (2810–2900 sec).

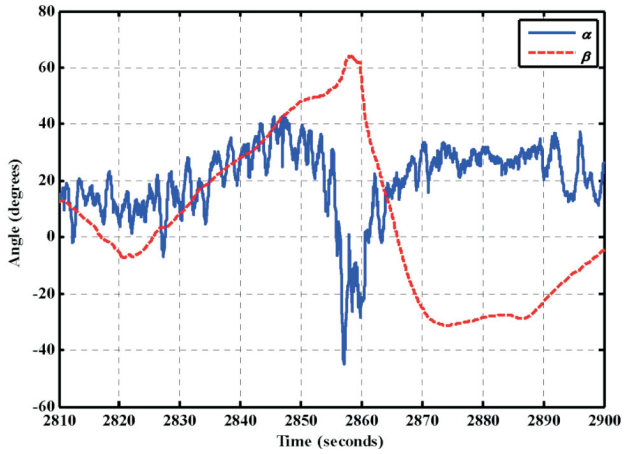

Figure 18. Angle of attack α and angle of sideslip β (2810–2900 sec).

man filter design for attitude estimation using low cost MEMS-based flight information measurement unit. The proposed attitude estimation algorithm is intuitive, easy to implement, and reliable for long-term high dynamic maneuvers. The algorithm utilized the evolution of the four elements of the quaternion method as the dynamical model for the Kalman filter. The pitch and roll angles computed from gravity force decomposition are considered as the measurement for the filter. In addition, the constraint of the four elements of the quaternion method is treated as a perfect measurement and is integrated into the system to form a constrained unscented Kalman filter. The immeasurable gravity accelerations are deduced from the outputs of the three axes accelerometers, the relative accelerations, and the accelerations due to body rotation. The heading angle is obtained from a complimentary filter. The complimentary filter uses the heading signal deduced from an electronic magnetic sensor and the GPS-derived heading as the inputs to achieve a long-term accurate, reliable and less noisy heading information. An experiment using an in-house designed motion platform is conducted to evaluate the proposed attitude estimation algorithm. The noise characteristics of the sensor signals are examined using the laboratory data. Approximations of the time-varying noise variances of the measured signals are obtained through Taylor series expansions. The proposed algorithm is successfully verified through a set of flight test data collected from the in house-designed MEMS-based attitude determination system.

Acknowledgement

This research is supported by the National Science Council, Taiwan, Republic of China, under Grant NSC 99-2212-E-032-012.

References

[1] Demoz, G. E., "A Low-Cost GPS/Inertial Attitude Heading Reference System (AHRS) for General Aviation Applications," *Proc. of IEEE 1998 Position Location and Navigation Symposium*, pp. 518–525 (1998). doi: 10.1109/PLANS.1998.670207

[2] Demoz, G. E., Elkaim, G. H., Powell, J. D. and Parkison, B. W., "A Gyro-Free Quaternion-Based Attitude Determination System Suitable for Implementation Using Low Cost Sensors," *Proc. of 2000 IEEE Position Location and Navigation Symposium*, pp. 185–192 (2000). doi: 10.1109/PLANS.2000.838301

[3] Wang, L., Xiong, S., Zhou, Z., Wei, Q. and Lan, J., "Constrained Filtering Method for MAV Attitude Determination," *Proc. of IEEE 2005 Instrumentation and Measurement Technology Conference*, pp. 1480–1483 (2005). doi: 10.1109/IMTC.2005.1604397

[4] Euston, M., Coote, P., Mahony, R., Kim, J. and Hamel, T., "A Complementary Filter for Attitude Estimation of a Fixed-Wing UAV," *Proc. of 2008 IROS, IEEE/RSJ International Conference on Intelligent Robots and Systems*, pp. 340–345 (2008). doi: 10.1109/IROS.2008.4650766

[5] Yoo, T. S., Hong, S. K., Yoon, H. M. and Pa, S.,

"Gain-Scheduled Complementary Filter Design for a MEMS Based Attitude and Heading Reference System", *Sensors*, Vol. 11, pp. 3816–3830 (2011). doi: 10.3390/s110403816

[6] Zhu, R., Sun, D., Zhou, Z. and Wang, D., "A Linear Fusion Algorithm for Attitude Determination Using Low Cost MEMS-Based Sensors," *Measurement*, Vol. 40, pp. 322–328 (2007). doi: 10.1016/j.measurement.2006.05.020

[7] Hong, S. K. "Fuzzy Logic Based Closed-Loop Strapdown Attitude System for Unmanned Aerial Vehicle (UAV)," *Sensors and Actuators A: Physical*, Vol. 107, pp. 109–118 (2003). doi: 10.1016/S0924-4247(03)00353-4

[8] Wang, M., Yang, Y., Ronald, R. H. and Zhang, Y., "Adaptive Filter for a Miniature MEMS Based Attitude and Heading Reference System," *Proc. of 2004 IEEE, Position Location and Navigation Symposium*, pp. 193–200 (2004). doi: 10.1109/PLANS.2004.1308993

[9] Lam, Q. M. and Crassidis, J. L., "Precision Attitude Determination Using a Multiple Model Adaptive Estimation Scheme," *Proc. of 2007 IEEE, Aerospace Conference*, pp. 1–20 (2007). doi: 10.1109/AERO.2007.352657

[10] Crassidis, J. L. and Markley, F. L., "Unscented Filtering for Spacecraft Attitude Estimation," *Journal of Guidance Control and Dynamics*, Vol. 26, No. 4, pp. 536–542 (2003). doi: 10.2514/2.5102

[11] Shin, E. H. and El-Sheimy, N., "An Unscented Kalman Filter for In-Motion Alignment of Low-Cost IMUs," *Proc. of 2004 Position Location and Navigation Symposium*, pp. 273–279 (2004). doi: 10.1109/PLANS.2004.1309005

[12] VanDyke, M. C., Schwartz, J. L. and Hall, C. D., "Unscented Kalman Filtering for Spacecraft Attitude State and Parameter Estimation," *Proc. of the AAS/AIAA Space Flight Mechanics Conference*, No. AAS 04-115 (2004).

[13] Zhao, L., Nie, Q. and Guo, Q., "Unscented Kalman Filtering for SINS Attitude Estimation," *Proc. of 2007 IEEE International Conference on Control and Automation*, pp. 228–232 (2007). doi: 10.1109/ICCA.2007.4376353

[14] Shiau, J.-K., Ma, D.-M., Wu, T.-H. and Huang, L.-H., "Design of a MEMS-Based Flight Information Measurement Unit for UAV Application", *Journal of Emerging Trends in Engineering and Applied Sciences*, Vol. 2, No. 2, pp. 197–204 (2011).

[15] Baruh, H., *Analytical Dynamics*, McGraw-Hill (1999).

[16] Collinson, R. P. G., *Introduction To Avionics*, CHAPMAN & HALL (1996).

[17] Simon, D., *Optimal State Estimation*, Wiley (2006).

Manuscript Received: Jun. 27, 2012
Accepted: Sep. 21, 2012